Supplementary Information:

A Route towards Digital Manipulation of Water Nanodroplets on Surface

Meng Cheng[1†], Duoming Wang[1†], Zhaoru Sun[2†], Jing Zhao[1], Rong Yang[1], Guole Wang[1], Wei Yang[1], Guibai Xie[1], Jing Zhang[1], Peng Chen[1], Congli He[1], Donghua Liu[1], Limei Xu[2], Dongxia Shi[1], Enge Wang[2] and Guangyu Zhang[1*]

[1] Beijing National Laboratory for Condensed Matter Physics and Institute of Physics, Chinese Academy of Sciences, Beijing 100190, China
[2] International Centre of Quantum Materials, School of Physics, Peking University, Beijing 100871, China

[†]These authors contributed equally to this work.
[*]Corresponding author. Email: gyzhang@aphy.iphy.ac.cn
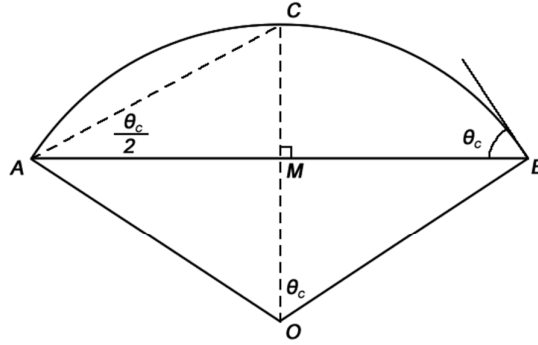
(1) Calculation of contact angle (θ_C)

  Here in Figure S1, AB is the diameter (D) and CM is the height (H) of the droplet. It is easy to notice that θ_C equals to $\angle COB$ and double $\angle CAM$, then

$$\tan \angle CAM = \tan \frac{\theta_C}{2} = \frac{CM}{AM} = \frac{H}{D/2}.$$

Thus we have $\theta_C(°) = 2 \cdot \arctan(\dfrac{2H(nm)}{D(nm)})$

Considering the linear relationship of H and D, $H = kD + b$

We got $\theta_C(°) = 2 \cdot \arctan(\dfrac{2k}{D(nm)} + 2b)$

Figure S1. A schematic for geometrical relationship between θ_C, D and H.

**(2) The elastic modules of the WNs in peak force mode.**

The elastic modules of the WNs were measured using peak-force mode of AFM (Dimension Edge, Bruker Inc. USA) since the mechanical information is lacking in previous studies. The following couple images, Derjaguin-Mueller-Toporov (DMT) modulus [1,2] signal (Figure S2a) and topography signal (Figure S2b), were captured from the same area in peak force mode simultaneously. From the cross section image (Figure S2a bottom), the DMT modulus of the center part of a droplet is found to be a constant basically. This flat bottom is the section where we estimate the DMT modulus for a droplet by taking average of. The corresponding topography image is somehow strange for there appears a ring-like platform.
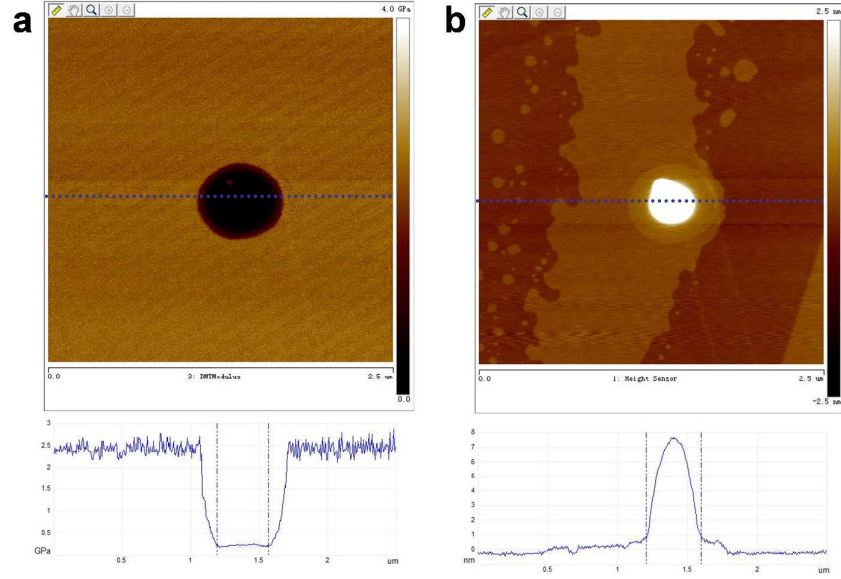
Figure S2. The topography image (a) and DMT modulus image (b) of the same droplet and in one scan. The bottom curves are the cross sections along the blue dotted lines, respectively.

## (3) Dependence of DMT modulus on WNs size

DMT modulus mapping image of the same area in Figure S3a is shown in Figure 1d. A significant difference in DMT modulus mapping is observed between regions with (~0.5 GPa) and without (~18.6 GPa) WNs underneath (Figure S3b). The reported elastic modulus of mica (along *c*-axis) and bulk water is ~171 and 2.2 GPa, respectively [3, 4]. The measured modulus may be not accurate and could vary in different experiments. However, the resulted ratio of DMT modulus between mica and trapped WNs gives 32.8, smaller than 77.7 in references, indicating the higher hardness of WNs in our samples possibly due to their higher internal pressure induced by graphene covering. Besides, the plot of the inverse DMT modulus as a function of *D* (Figure 1e) reveals a proportional relationship, which is related to the different curvatures of WNs.[5]
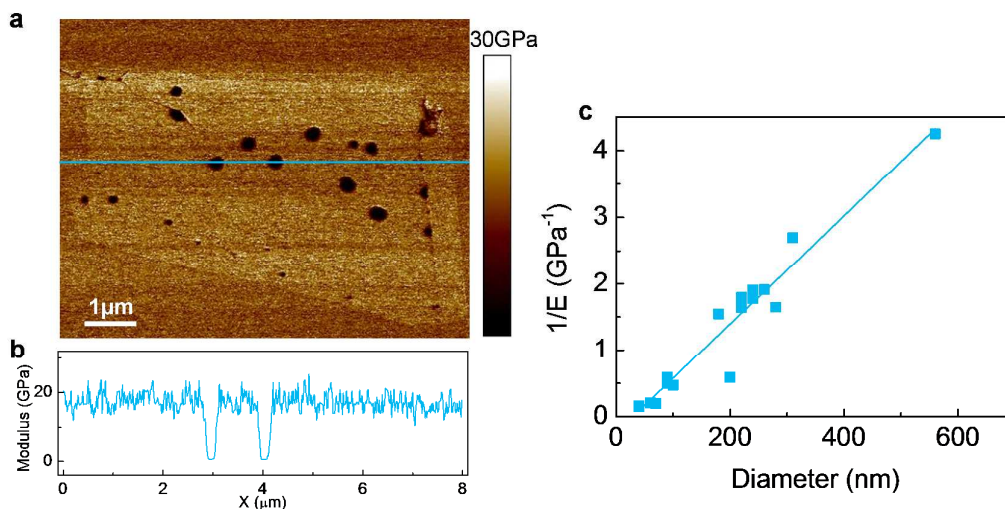
Figure S3. (a) DMT modulus mapping image of same area in Figure 1a. Those black areas correspond to WNs. (b) The cross section along the blue line. (c) Plot of the inverse of the DMT modulus of WNs as a function of different diameters, which can be linear fitted.

(4) Cross section of water-drop in contact mode with different setpoints.

We acquire the cross sections with f_{tip} from 20 nN to 240 nN and show the curves here with different colors for distinguish (Figure S4). It is reasonable that the height and lateral size are both depressed by the heavy tip-induced press. Like the topography image in peak force mode, there is also a halo layer, which can be thought as the bottom of the nanodroplet. The bottom layer, highlighted by dark green, is stable while pressing, whose thickness is about 0.4 nm, close to that of monolayer ice.
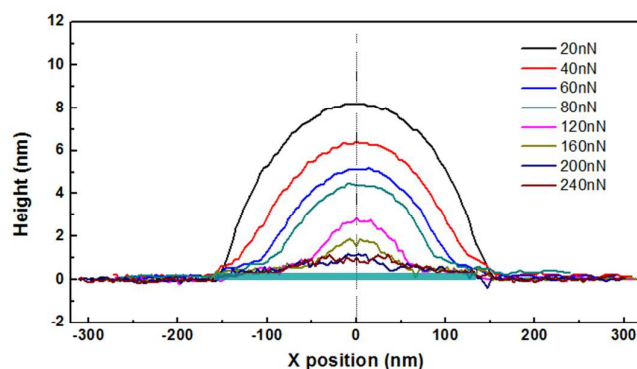
Figure S4. A serial of cross sections with different setpoints, from 20 nN to 200 nN,

corresponding to Figure 3a to 3h.

References:

S1.   Derjaguin, B. V.; Muller, V. M.; Toporov, Y. P. Effect of Contact Deformations on the Adhesion of Particles. *J. Colloid Interface Sci.* **1975**, *53*, 314-326.

S2.   Muller, V. M.; Derjaguin, B. V.; Toporov, Y. P. On 2 Methods of Calculation of the Force of Sticking of an Elastic Sphere to a Rigid Plane. *Colloid Surf.* **1983**, *7*, 251-259.

S3.   Kracke, B.; Damaschke, B. Measurement of Nanohardness and Nanoelasticity of Thin Gold Films with Scanning Force Microscope. *Appl. Phys. Lett.* **2000**, *77*, 361-363.

S4.   Weir, S. T.; Chandler, E. A.; Goodwin, B. T. Rayleigh-Taylor Instability Experiments Examining Feedthrough Growth in an Incompressible, Convergent Geometry. *Phys. Rev. Lett.* **1998**, *80*, 3763-3766.

S5.   Mendez-Vilas, A.; Jodar-Reyes, A. B.; Gonzalez-Martin, M. L. Ultrasmall Liquid Droplets on Solid Surfaces: Production, Imaging, and Relevance for Current Wetting Research. *Small* **2009**, *5*, 1366-1390.